This self-consistent equation is the same as the one Taylor obtained by another method as can be seen by multiplying both sides by $(1+\Sigma D_0)^{-1}[1+\Sigma D_0-(1-c)$ $\times M_A \epsilon \omega^2 D_0]$ to obtain

$$\Sigma(1+\Sigma D_0)^{-1}[1+\Sigma D_0-(1-c)M_A \epsilon \omega^2 D_0]=cM_A \epsilon \omega^2, \quad (14)$$

which is Eq. (3.7) of Taylor's paper.[1]

It now seems, with Taylor's calculations and this connection with the usual diagrams, that implicit compensation in diagrams is important. Furthermore,

Yonezawa and Matsubara[12] have pointed out that any theory at large concentrations should be symmetric in the A- and B-atom types. Taylor has shown that Eq. (14) has this symmetry, so that implicit compensation also seems to restore A-B atom symmetry. A further feature of this method is that, with the resulting implicit equations in any calculation, the perturbation expansion is no longer a power series in c and can possibly yield results that are not analytic at $c=0$.

[12] F. Yonezawa and T. Matsubara, Progr. Theoret. Phys. (Kyoto) **35**, 357 (1966).

Lattice Dynamics of Niobium-Molybdenum Alloys

B. M. Powell, P. Martel, and A. D. B. Woods

Chalk River Nuclear Laboratories, Chalk River, Ontario, Canada

(Received 11 January 1968)

The frequency-versus-wave-vector dispersion relations for the normal modes of vibration of a series of alloys of the transition metals niobium and molybdenum have been measured at 296°K, and previous measurements on the pure metals have been extended, using coherent, one-phonon scattering of thermal neutrons. The phonon dispersion relations are very different for the two pure metals, suggesting that the electronic structure, acting through the electron-phonon interaction, plays a significant role in the determination of the dynamics of these materials. The observed neutron groups corresponding to the phonons in the alloys are not significantly broader than in the pure metals. The dependence of the dispersion curves on alloy composition is found to be complicated, both the general level of frequencies and the shape of the curves changing significantly. Fourier analysis indicates that the interatomic forces in the metals are oscillatory and of long range. Suspected Kohn anomalies are observed on several branches of the dispersion curves. With the assumption of a rigid-band model, the positions of several of these anomalies correlate with the calculated electron band structure for tungsten. The dimensions of the Fermi surface obtained from this correlation are in agreement with other Fermi-surface information.

1. INTRODUCTION

TRANSITION metals are characterized by a partially filled inner electronic shell. This unfilled shell results in many unusual properties[1] and might be expected to have a significant effect on the interatomic force system. This paper presents extensive measurements of the phonon dispersion curves of niobium and molybdenum and their alloys which demonstrate that such effects are quite marked. In favorable cases the results can yield information concerning the details of the electronic band structure.

The dispersion curves of the column-V transition metals niobium[2] (in the 4d series) and tantalum[3] (5d) show many similarities, as do those of the column-VI metals chromium[4] (3d), molybdenum[5] (4d), and tung-

sten[6] (5d). The dispersion curves of the column-V metals, however, differ greatly, both in shape and frequency level, from those of the column-VI metals.[7] Such effects imply a strong dependence of the interatomic forces on the electronic structure for these metals. Measurements of the dispersion curves of other metals[8] indicate that the interatomic forces in some are complicated while in others they are comparatively simple.

The electronic structures of the column-V and column-VI metals differ in that the column-V metals have five electrons outside the closed shell and the column-VI metals, six. Consequently, measurements of the phonon dispersion curves of a series of binary alloys of metals in columns V and VI in the same row should provide information on how the addition of d electrons to the unfilled shell changes the normal modes of vi-

[1] For a review of the properties of transition metals see S. V. Vonsovskii and Yu. A. Izyumov, Usp. Fiz. Nauk **77**, 377 (1962) [English transl.: Soviet Phys.—Usp. **5**, 547 (1963)].

[2] Y. Nakagawa and A. D. B. Woods, in *Lattice Dynamics*, edited by R. F. Wallis (Pergamon Press, Ltd., Oxford, England, 1965), p. 39; Phys. Rev. Letters **11**, 271 (1963).

[3] A. D. B. Woods, Phys. Rev. **136**, A787 (1964).

[4] H. Bjerrum Møller and A. R. Mackintosh, in *Inelastic Scattering of Neutrons in Solids and Liquids* (International Atomic Energy Agency, Vienna, 1965), Vol. I, p. 95.

[5] A. D. B. Woods and S. H. Chen, Solid State Commun. **2**, 233 (1964).

[6] S. H. Chen and B. N. Brockhouse, Solid State Commun. **2**, 73 (1964).

[7] A. D. B. Woods and B. M. Powell, Phys. Rev. Letters **15**, 778 (1965); see also A. D. B. Woods, Brookhaven National Laboratory Report No. 940(c-45), 1965, p. 8 (unpublished).

[8] For general reviews of previous measurements of $\nu(q)$ for metals see G. Dolling and A. D. B. Woods, in *Thermal Neutron Scattering*, edited by P. A. Egelstaff (Academic Press Inc., New York, 1965), Chap. 5; B. N. Brockhouse, in *Phonons*, edited by R. W. H. Stevenson (Oliver and Boyd, Ltd., Edinburgh, 1966), Chap. 4.

bration and, hence, the interatomic force system. The alloy system chosen for these experiments was the niobium-molybdenum (Nb-Mo) system, both metals belonging to the 4d series. The pure metals have excellent neutron properties and extensive measurements of their dispersion relations have already been made.[2,5] The metals form a complete series of disordered solid solutions, all having a body-centered cubic structure, thus permitting intercomparisons to be readily made. Preliminary results of these measurements have been published.[7] Similar experiments[9] have recently been done on the Bi-Pb-Tl alloy system and, using incoherent scattering, on powdered vanadium alloys.

2. EXPERIMENTAL DETAILS

Experiments were carried out on six alloys of various compositions. In addition, some measurements were made on a crystal of niobium containing about 4% zirconium. The alloy compositions were checked by measuring the lattice spacing with neutron diffraction methods, and comparing the measured lattice spacings with the published values for this alloy system.[10] The single-crystal specimens of both pure metals and alloys were in the form of cylinders, the cylinder base being approximately parallel to a (110)-type plane. With the cylinder axis horizontal the mosaic spread about the vertical axis of all the single-crystal specimens was approximately 0.5°. The specimens for the pure metals consisted of three such cylinders, each approximately 5 cm long×1 cm diam. The niobium crystals were obtained from Metals Research Ltd., Cambridge, England and the molybdenum crystals were supplied by Linde

Co., through Union Carbide (Canada) Ltd. The alloy specimens, supplied by Materials Research Corporation, were of various sizes.

The measurements were made at a temperature of 296°K on the triple-axis spectrometer[11] at the NRU reactor. The experiment was carried out using the spectrometer in its constant Q mode of operation and with variable incident energy. The crystals were mounted so that a (110) plane was horizontal. With this orientation measurements could be made along the symmetry directions Δ, Σ, and $\Lambda(F)$ (in previous notation [00ζ], [$\zeta\zeta$0], and [$\zeta\zeta\zeta$], respectively).

3. EXPERIMENTAL RESULTS

The normal mode frequencies (ν) measured as a function of phonon wave-vector (q) for the Nb-Mo system are shown in Figs. 1–8. The straight lines through the origin in Figs. 1 and 8 are the velocity of sound lines calculated from the measured elastic constants of niobium[12] and molybdenum,[13] respectively. The experimental accuracy in the phonon energy determination was typically about 2%.

The differences between the phonon dispersion curves of the two pure metals niobium and molybdenum[2,5,14] can be seen by comparing Figs. 1 and 8. The shapes of the curves are very different and, on average, the frequencies of modes in molybdenum are significantly higher ($\sim$25%) than in niobium. Several anomalies can be seen for each metal. The most striking of these occur on the Λ_1 branches near the point P in niobium and near H in molybdenum. The possible connection between
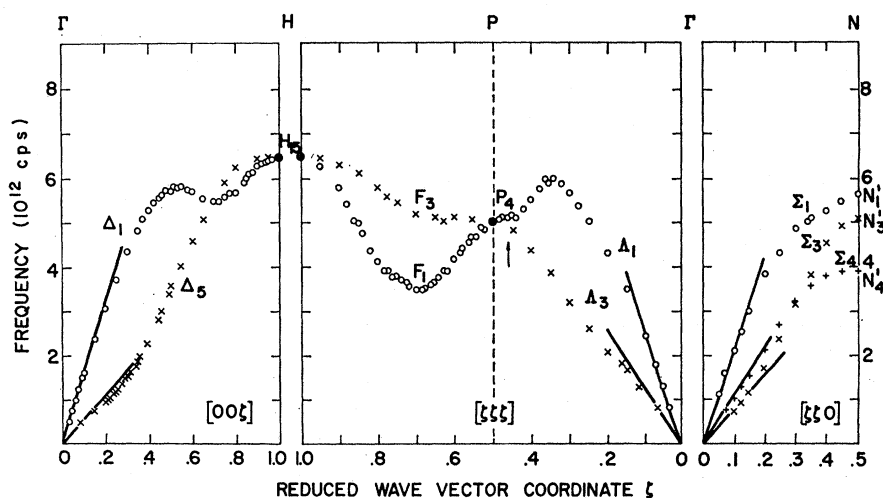
FIG. 1. Dispersion curves of niobium. The arrow indicates the position of the anomaly discussed in the text.

[9] S. C. Ng and B. N. Brockhouse, Solid State Commun. 5, 79 (1967); B. Mozer, K. Otnes and C. Thaper, Phys. Rev. 153, 535 (1966).
[10] W. B. Pearson, *Handbook of Lattice Spacings and Structures of Metals* (Pergamon Press, Inc., New York, 1958).
[11] B. N. Brockhouse, in *Inelastic Scattering of Neutrons in Solids and Liquids* (International Atomic Energy Agency, Vienna, 1961), p. 113.
[12] R. J. Wasilewski, J. Phys. Chem. Solids 26, 1643 (1965).
[13] F. H. Featherstone and J. R. Neighbours, Phys. Rev. 130, 1324 (1963).
[14] A. D. B. Woods, in *Inelastic Scattering of Neutrons in Solids and Liquids* (International Atomic Energy Agency, Vienna, 1965), Vol. I, p. 87.

FIG. 2. Dispersion curves of
$Nb_{0.85}$–$Mo_{0.15}$.
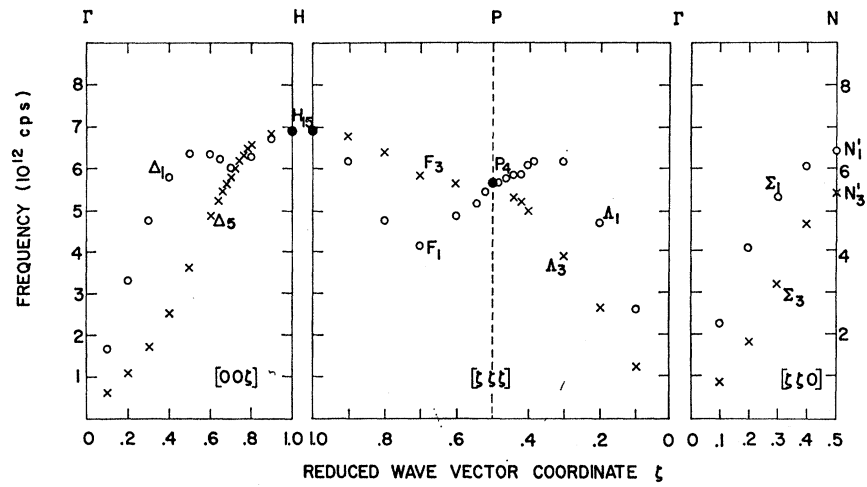
FIG. 3. Dispersion curves of
$Nb_{0.65}$-$Mo_{0.35}$.
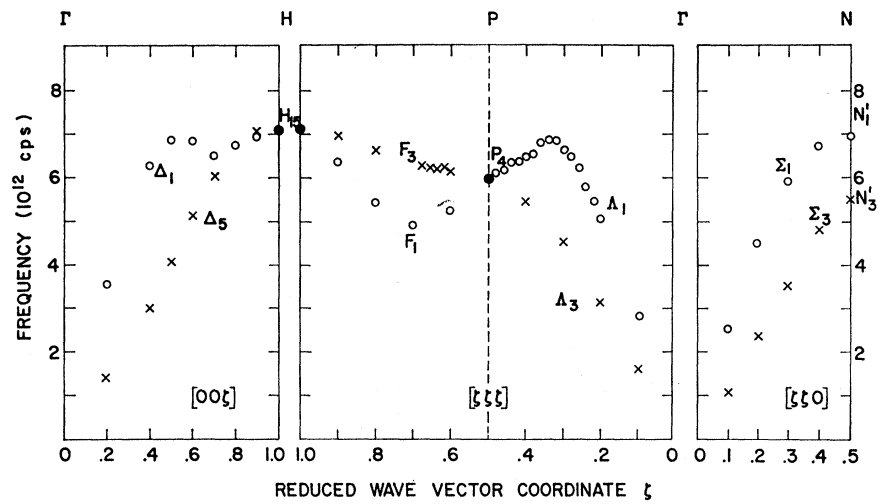
FIG. 4. Dispersion curves of
$Nb_{0.59}$-$Mo_{0.41}$.
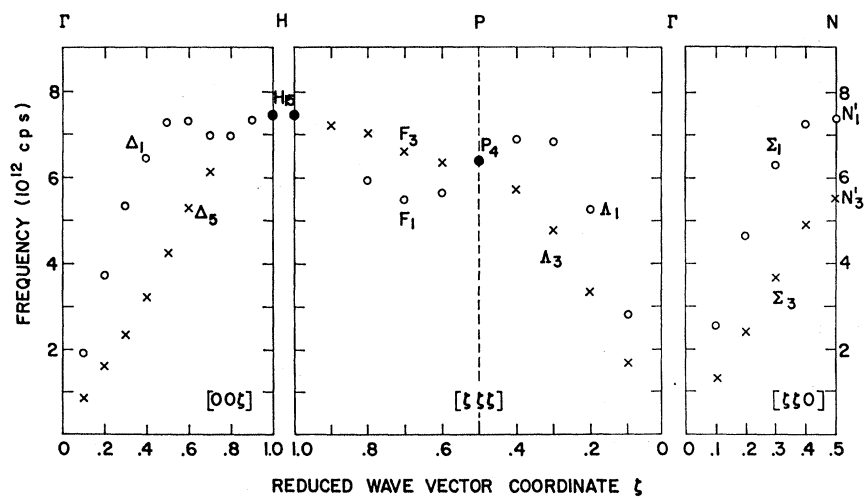
these and other anomalies and the electronic structure will be discussed below.

The phonon dispersion curves of the Nb-rich alloys $Nb_{0.85}$-$Mo_{0.15}$, $Nb_{0.65}$-$Mo_{0.35}$, and $Nb_{0.59}$-$Mo_{0.41}$ are shown in Figs. 2–4. The curves show a shape remarkably similar to those of pure niobium, but the general fre-
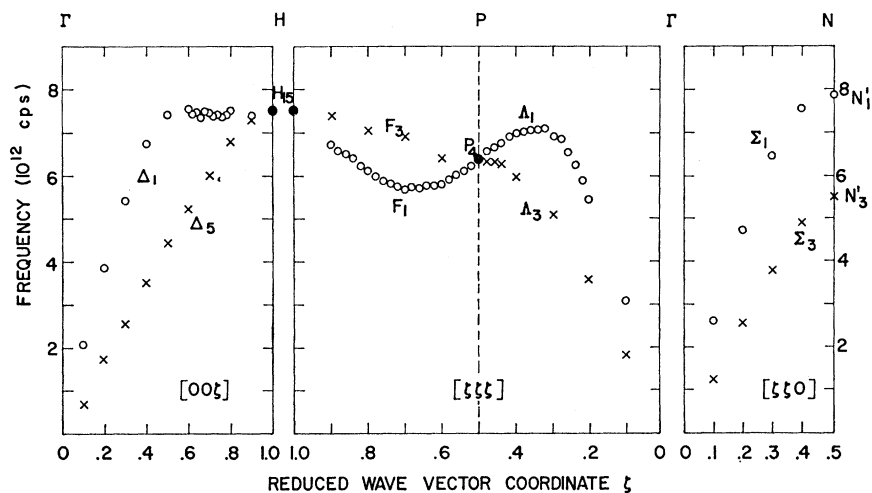
FIG. 5. Dispersion curves of
$Nb_{0.44}$-$Mo_{0.56}$.
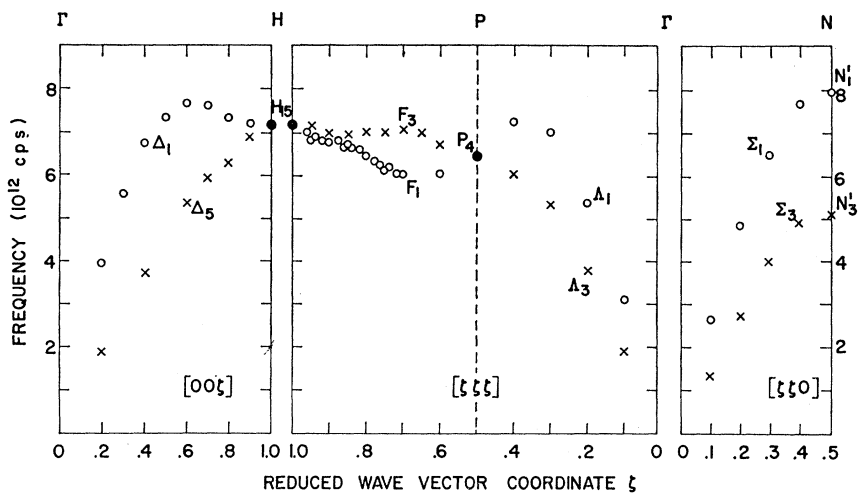
FIG. 6. Dispersion curves of
$Nb_{0.25}$-$Mo_{0.75}$.
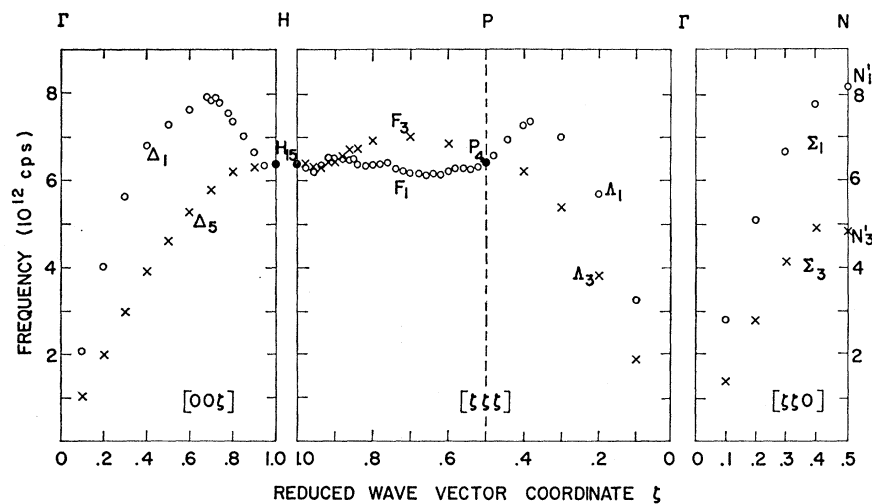
FIG. 7. Dispersion curves of
$Nb_{0.09}$-$Mo_{0.91}$.

quency level increases with molybdenum content. On the Δ_1 branches the positions of the local maximum and minimum show little change with composition. The un-

usual shape of the Δ_5 branch at small q and the intersection of the Δ_1 and Δ_5 branches disappear with increasing molybdenum content. The frequency of the

FIG. 8. Dispersion curves of molybdenum. The arrows indicate the positions of anomalies discussed in the text.
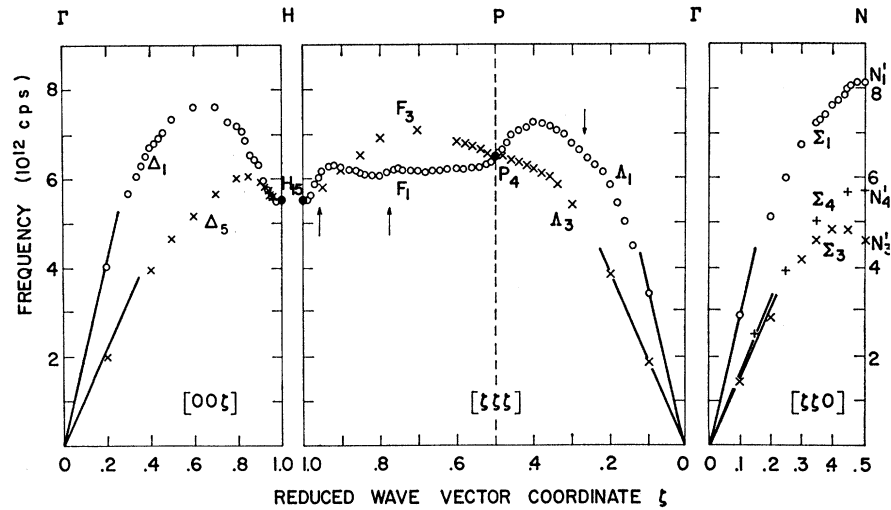
N_1' mode shows a large change with composition, but the N_3' mode is almost constant. The deep minimum, evident on the F_1 branch of pure niobium, becomes less pronounced as the molybdenum content increases. The anomaly near P on the Λ_1 branch in pure niobium persists in the alloys, but moves to smaller values of ζ and becomes gradually weaker as the molybdenum content increases.

Figure 5 shows the dispersion curves of the alloy $Nb_{0.44}$-$Mo_{0.56}$. The shapes of these curves appear to be intermediate between those of the pure metals. Pronounced anomalies are no longer observable, and the dispersion curves are remarkably smooth.

The phonon dispersion curves of the Mo-rich alloys $Nb_{0.25}$-$Mo_{0.75}$ and $Nb_{0.09}$-$Mo_{0.91}$ are shown in Figs. 6 and 7. The frequencies are similar to those of pure molybdenum. The Λ_1, Λ_3, and Σ_1 branches in these alloys are almost identical to those in pure molybdenum while the Δ_1, Δ_5, and Σ_3 branches differ from the respective branches in pure molybdenum only near the zone boundary. In this region the decrease in frequency, present on all these branches, increases with molybdenum content. Differences between the F_1 and F_3 branches in the alloys and in pure molybdenum are also most pronounced near H. The small kink at $\zeta \sim 0.78$ on the F_1 branch in pure molybdenum is observed at approximately the same ζ value in $Nb_{0.09}$-$Mo_{0.91}$. It is weaker in this alloy and it is too small to be seen in $Nb_{0.25}$-$Mo_{0.75}$. The very pronounced anomaly at $\zeta \sim 0.96$ on the F_1 branch in pure molybdenum becomes progressively weaker as the molybdenum content decreases, and its position moves to smaller values of ζ.

This fine structure is believed to be real since it is reproducible under varying conditions of resolution and in different positions in reciprocal space. Other apparent irregularities, such as occur on the Δ_1 branch of the $Nb_{0.44}$-$Mo_{0.56}$ alloy (Fig. 5) are not well established and are not considered significant.

The variation of frequency with composition for

several special modes is shown in Fig. 9. It can be seen that for the Nb-rich alloys all of these frequencies increase with molybdenum content until approximately equiatomic composition is reached. The frequencies of the N_1' and P_4 modes are then almost constant with further increase of the molybdenum content, while those of the N_3' and H_{15} modes decrease. This decrease is very marked in the case of the H_{15} mode.

The constituent atoms in this alloy system have similar masses (for niobium $M = 92.91$, for molybdenum $M = 95.94$), thus effects due to mass disorder in the alloys are expected to be negligible. However, the very different phonon dispersion relations for niobium and
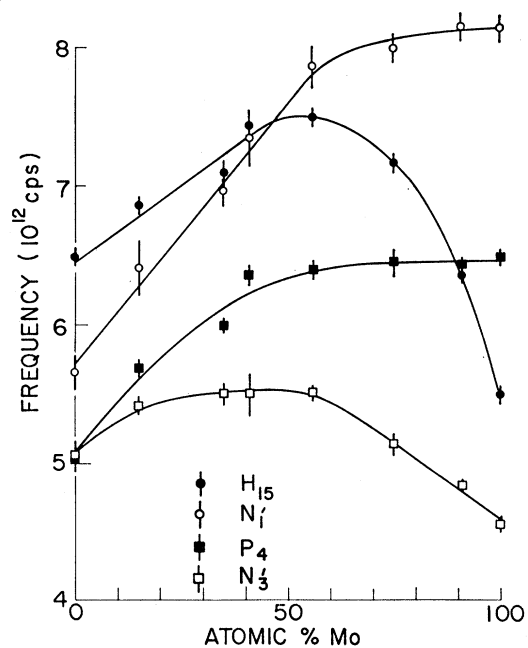
FIG. 9. Frequency variation of some zone boundary modes as a function of composition in Nb-Mo alloys.

TABLE I. Fourier coefficients Φ_n (units of 10^3 dyn cm^{-1}), for various branches of the dispersion relations of Nb-Mo alloys.

	Φ_1	Φ_2	Φ_3	Φ_4	Φ_5	Φ_6	Φ_7	Φ_8	Φ_9	Φ_{10}	Φ_{11}	Φ_{12}	Φ_{13}	Φ_{14}	Φ_{15}	Φ_{16}
Niobium																
Δ_1	100.93	35.37	24.64	-13.93	2.48	1.80	-0.40	-0.65	1.00	-0.24	-3.35	-1.43	-0.92	0.98	1.28	0.83
Δ_5	135.85	-28.41	-6.50	5.01	-1.50	1.70	-0.72	0.48	5.47	2.67						
$\Lambda_1(F_1)$	35.87	17.10	82.06	-8.64	10.57	-8.11	-2.70	0.77								
$\Lambda_3(F_3)$	113.09	8.91	16.37	-14.47	-1.95	4.38	0.06	-0.34	1.10	-0.84	-0.93	1.00				
Σ_1	91.27	11.37	2.49	-2.03	2.17	-2.49	1.43	-0.09								
Σ_3	75.23	-21.56	3.03													
Nb$_{0.85}$-Mo$_{0.15}$																
Δ_1	118.96	49.05	26.23	-16.56	2.64	2.04	-2.45	0.93	1.19	-0.52						
Δ_5	151.96	-32.26	-6.41	5.49	-0.69	-0.14	-0.01	-0.05	1.03	2.91						
$\Lambda_1(F_1)$	46.70	27.34	89.73	-7.06	12.30	-8.33	-5.64	-0.59	0.08	0.34	1.80					
$\Lambda_3(F_3)$	129.98	19.93	19.48	-11.51	-3.34	4.28	-0.20	-1.67								
Σ_1	120.52	7.57	3.99	-2.02	1.12											
Σ_3	82.33	-25.23	6.23	-1.98	0.93											
Nb$_{0.65}$-Mo$_{0.35}$																
Δ_1	130.43	64.27	24.22	-17.07	0.39	3.71										
Δ_5	160.90	-28.49	-4.76	3.53	-0.50	1.23										
$\Lambda_1(F_1)$	51.96	39.84	92.02	3.79	8.33	-8.91	-3.31	0.45	1.98	1.78	4.26	-5.18				
$\Lambda_3(F_3)$	136.09	32.81	20.52	-6.96	-0.44	0.29	-0.88									
Σ_1	148.92	11.33	0.43	0.80	0.26											
Σ_3	86.94	-20.17	6.66	-2.35	-0.11											
Nb$_{0.59}$-Mo$_{0.41}$																
Δ_1	146.52	73.67	22.01	-18.40	5.67	1.97	-3.41	1.35								
Δ_5	170.72	-30.88	0.31	1.83	0.65	-5.99										
$\Lambda_1(F_1)$	70.66	44.71	96.49	2.64	3.62											
$\Lambda_3(F_3)$	148.27	36.48	23.12	-7.93	-0.84											
Σ_1	171.79	9.41	-3.91	4.42	-1.19											
Σ_3	86.81	-18.75	5.29	-1.43	1.23											
Nb$_{0.44}$-Mo$_{0.56}$																
Δ_1	158.44	81.15	15.45	-9.78	-1.19	3.49	-0.65	-1.23	2.89	-0.38						
Δ_5	168.30	-28.0	7.24	-2.97	0.11	1.60	1.01	-3.12	-2.92	3.23						
$\Lambda_1(F_1)$	67.42	49.25	91.85	11.63	7.15	-7.63	4.49	-2.93			3.44	-1.50	5.02	-1.38		
$\Lambda_3(F_3)$	150.13	39.21	27.20	-0.69	-4.52	-2.70										
Σ_1	192.68	2.79	-0.46	2.85	-0.19											
Σ_3	88.65	-15.05	4.96	-2.50	0.52											
Nb$_{0.25}$-Mo$_{0.75}$																
Δ_1	152.39	91.61	6.20	-0.78	0.22	-2.56	0.39	4.14	4.58	-2.87	3.62					
Δ_5	149.35	-12.45	6.36	-4.27	5.05	-4.87	2.56	-3.03	-2.71	0.88						
$\Lambda_1(F_1)$	71.72	59.69	85.35	18.83	-4.50	-6.84	1.80									
$\Lambda_3(F_3)$	139.44	55.49	17.78	6.74	0.35	-7.16										
Σ_1	199.11	1.99	2.18	3.24	-1.65											
Σ_3	84.66	-5.42	-1.89	1.27	-0.36											

TABLE I (continued).

	Φ_1	Φ_2	Φ_3	Φ_4	Φ_5	Φ_6	Φ_7	Φ_8	Φ_9	Φ_{10}	Φ_{11}	Φ_{12}	Φ_{13}	Φ_{14}	Φ_{15}	Φ_{16}	Φ_{17}	Φ_{18}	Φ_{19}	Φ_{20}
$Nb_{0.09}$-$Mo_{0.91}$																				
Δ_1	138.57	107.04	−8.74	16.03	−7.68	−4.03	5.42	−0.620	−1.08											
Δ_5	129.81	3.44	−1.26	1.12	−1.93	0.67														
$\Delta_1(F_1)$	56.42	71.70	72.33	31.21	−3.21	−3.20	0.62	7.17	2.68	−2.31	−3.90									
$\Delta_3(F_3)$	122.22	73.45	8.33	14.84	−6.21	−4.71	−0.21	0.58	−3.84	−2.03	6.36									
Σ_1	202.66	6.78	6.33	0	−0.72															
Σ_3	81.37	0.92	−6.55	4.01	−1.37															
Molybdenum																				
Δ_1	119.19	117.42	−12.99	16.94	−8.04	3.15	−3.48	6.94	−6.32	−0.27	−4.09	5.28	−3.00	2.62	−0.22	2.52	−1.18	0.52	−1.80	1.53
Δ_5	114.38	14.49	−9.46	5.71	−8.04	6.04	4.38	−0.08	−0.05	1.01	−1.77	2.09								
$\Delta_1(F_1)$	45.40	78.38	63.56	29.15	−1.66	2.28	−2.56													
$\Delta_3(F_3)$	112.32	85.01	−0.42	22.47	−11.91	−0.88														
Σ_1	198.31	11.13	6.35	−2.30	4.03	−2.30														
Σ_3	76.41	4.89	−8.07	5.42	−2.44															

molybdenum imply widely differing interatomic force systems in the two metals. Disordered alloys of the metals might therefore be expected to show effects due to force constant disorder. As reported previously,[7] no effects of this type have been observed in the widths of the neutron groups suggesting that to this degree of approximation, at least, these alloys may be considered to have ordered electronic and phonon structures, analogous in this respect to pure metals. However, the dispersion curves of the alloys near the equiatomic composition are smooth, showing no pronounced anomalies, and the intersection of various branches which occurs in the pure metals is absent. It is possible that these effects are connected with the atomic disorder.

A limited number of measurements were also made on the alloy $Zr_{0.04}$-$Nb_{0.96}$. Because of the low zirconium content, however, it was not possible to observe any significant differences between the dispersion curves of the alloy and the pure metal.

4. DISCUSSION

A. Fourier Analysis

To obtain information on the range of the interatomic forces in these metals, the individual branches of the dispersion relations have been fitted to a Fourier series. For the high-symmetry directions of simple materials (one atom in the primitive unit cell) the normal-mode frequencies can be expressed in the form[15,16]

$$4\pi^2 M\nu^2 = \sum_{n=1}^{N} \Phi_n \left(1 - \cos\frac{n\pi\zeta}{\zeta_{max}}\right), \tag{1}$$

where ν is the normal-mode freuqency, M the mass of the atom, and ζ the reduced wave-vector coordinate. The Fourier coefficients Φ_n, usually called interplanar force constants, are linear combinations of Born–von Kármán interatomic force constants. The Fourier coefficients for the symmetry directions of the pure metals and alloys are shown in Table I. The coefficients Φ_n have a complicated variation, as functions both of composition and of plane number n, reflecting the complicated nature of the individual dispersion curves and of their change with composition. The similarity in the shapes of the dispersion curves of the Nb-rich alloys and of pure niobium is borne out by the similar variation of their Fourier coefficients as a function of n. A corresponding pattern is not observed for the Mo-rich alloys, and this reflects the difference in the detailed shapes of the dispersion curves of pure molybdenum and these alloys.

The presence of unusual anomalies on several dispersion curves is reflected in the very high Fourier coefficients necessary to achieve a satisfactory fit to the

[15] A. J. E. Foreman and W. M. Lomer, Proc. Phys. Soc. (London) B70, 1143 (1957).

[16] B. N. Brockhouse, T. Arase, G. Caglioti, K. R. Rao, and A. D. B. Woods, Phys. Rev. 128, 1099 (1962).

observations, particularly for the $\Lambda_1(F_1)$ branches where the measurements are most detailed. These high coefficients imply that the interatomic forces are of very long range; for example, a significant value of Φ_{12} for the $\Lambda(F)$ branches shows that the forces extend to at least 13th nearest neighbors. In addition to their long range, the Fourier coefficients display an oscillatory behavior as a function of n. Koenig[17] has related such behavior to the long range Friedel oscillations[18] in the ion-ion potential. For the simple case of free electrons the period of the oscillations in the Fourier coefficients is directly related to $2k_F$, the diameter of the Fermi sphere. In these more complex transition metals the oscillations do not appear to have any single period which can be related to the Fermi surface dimensions. It should be noted that although the dispersion curves of the alloys near equiatomic composition are surprisingly smooth, the magnitudes of the long-range Fourier coefficients ($n \sim 12$) are not reduced by a large factor.

B. Comparison with Electronic Band Structure

Several authors[19-21] have carried out electron-band-structure calculations for the column-VI transition metals. These calculations appear to be reliable since the Fermi surfaces determined from them are supported by measurements[22] on both tungsten and molybdenum. Calculations for the 3d transition metals[23] and experiments on the high-field galvanomagnetic properties of niobium and tantalum[24] suggest that the rigid-band model is reasonable for these metals. If this assumption is made, the calculated band structure of Mattheiss[20] for tungsten, shown in Fig. 10, applies to niobium, molybdenum, and their alloys, and many of the features of the measured phonon dispersion curves can be correlated, at least qualitatively, with this band structure and the corresponding Fermi surfaces.

It can be seen from the measured dispersion curves that the general frequency level in the Nb-rich alloys rises with increasing molybdenum content. Over the same composition range the calculated electronic density of states at the Fermi surface, $N(E_F)$, shows a large decrease.[20] In the free-electron approximation, the

velocity of long-wavelength longitudinal sound waves[25] is proportional to $[N(E_F)]^{-1/2}$. If it is assumed that a similar expression holds for more complex metals and that the long-wavelength sound velocity is indicative of the general frequency level, the observed correlation can be qualitatively understood.

The oscillations of the Fourier coefficients Φ_n discussed in Sec. 4 A are related to a singularity in the electron dielectric function, which has a direct effect on the shapes of the dispersion curves. It was pointed out by Kohn[26] that when the phonon wave vector is equal to an extremal dimension across the Fermi surface, the phonon dispersion curves have an infinite slope, giving rise to a sharp kink or anomaly at this wave vector. The effect occurs when

$$\mathbf{Q}=2\pi\boldsymbol{\tau}+\mathbf{q}=\mathbf{k}_1-\mathbf{k}_2,$$

where $\mathbf{k}_1$, $\mathbf{k}_2$ are electron wave vectors on parallel sections of the Fermi surface, $\boldsymbol{\tau}$ is a reciprocal lattice vector, and $\mathbf{q}$ is the phonon wave vector. As described in Sec. 3, several well-defined anomalies are observed on various branches of the dispersion curves. Because of the finite resolution of the spectrometer, it cannot be unambiguously determined if these anomalies are the singularities expected from the Kohn effect. However, since several of them correlate with our present knowledge of the Fermi surfaces of these metals it is felt that this is the correct explanation at least in these cases.

With the assumption of rigid electron bands, changes in the Fermi surface with alloy composition arise from changes in the Fermi level relative to these rigid bands. The Fermi levels of the pure metals and of two alloys calculated[20] assuming all the electrons outside the closed shell to be valence electrons are shown in Fig. 10. The (110) sections of the resulting Fermi surfaces of niobium and molybdenum in the repeated reduced zone scheme are shown in Fig. 11.

The anomaly at $\zeta=0.46$ on the Λ_1 branch in Fig. 1 is believed to arise from electron transitions a-b across the niobium hole surface at H in Fig. 11. If this interpretation is correct, the radius of this hole surface in the [111] direction is 0.76 Å^{-1} compared with a calculated value of 0.67 Å^{-1}. Another possibility is that this anomaly may arise from transitions c-d across the hole surface at Γ. The calculated radius of this latter surface in the [111] direction is, however, only 0.43 Å^{-1}, and thus the possibility of the anomaly arising from this transition is less likely. The anomalies on the Λ_1 branches of the dispersion curves of the Nb-rich alloys, shown in Figs. 2 and 3, become weaker, and their positions move to progressively smaller values of ζ as the molybdenum content increases. In Fig. 10 it can be seen that the H hole surface arises from the intersection of the Fermi level with the F_1 electron bands, and that its radius in the [111] direction decreases with increasing molybdenum con-

[17] S. H. Koenig, Phys. Rev. 135, A1693 (1964).

[18] J. Friedel, Nuovo Cimento, Suppl. 2, 287 (1958).

[19] W. M. Lomer, Proc. Phys. Soc. (London) 80, 489 (1962); see also W. M. Lomer, ibid. 84, 327 (1964).

[20] L. F. Mattheiss, Phys. Rev. 139, A1893 (1965).

[21] T. L. Loucks, Phys. Rev. 139, A1181 (1965).

[22] G. B. Brandt and J. A. Rayne, Phys. Rev. 132, 1945 (1963); W. M. Walsh, Jr., and C. C. Grimes, Phys. Rev. Letters 13, 523 (1964); J. A. Rayne, Phys. Rev. 133, A1104 (1964); C. K. Jones and J. A. Rayne, in Proceedings of the Ninth International Conference on Low Temperature Physics (Plenum Press, Inc., New York, 1965), p. 790; W. M. Walsh, Jr., C. C. Grimes, G. Adams and L. W. Rupp, Jr., ibid., p. 765; D. M. Sparlin and J. A. Marcus, Phys. Rev. 144, 484 (1966); P. A. Bezuglyi, S. E. Zhevago, and V. I. Densisenko, Zh. Eksperim. i Teor. Fiz. 49, 1457 (1965) [English transl.: Soviet Phys.—JETP 22, 1002 (1966)].

[23] L. F. Mattheiss, Phys. Rev. 134, A970 (1964).

[24] E. Fawcett, W. A. Reed, and R. R. Soden, Phys. Rev. 159, 533 (1967).

[25] D. Bohm and T. Staver, Phys. Rev. 84, 836 (1952).

[26] W. Kohn, Phys. Rev. Letters 2, 393 (1959).
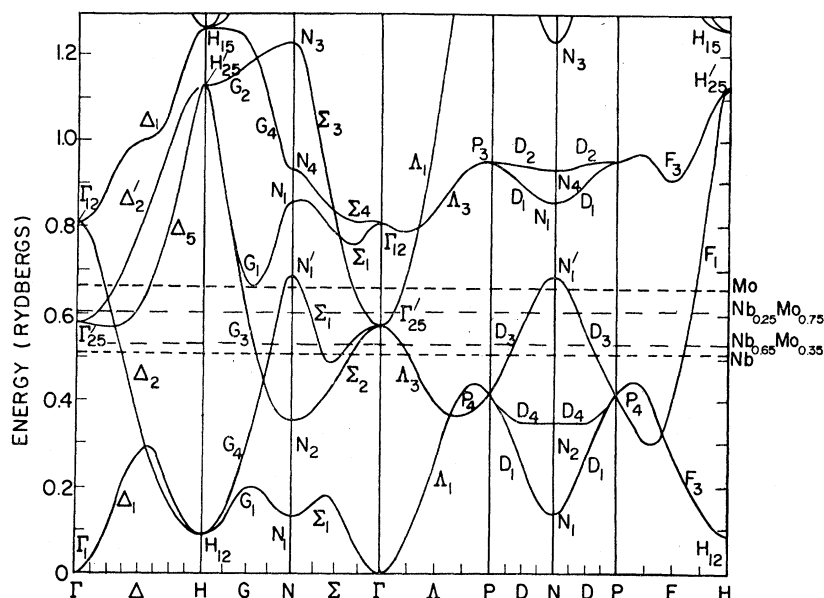
FIG. 10. Calculated electronic band structure for tungsten (see Ref. 20). The Fermi levels of niobium, $Nb_{0.65}$-$Mo_{0.35}$, $Nb_{0.25}$-$Mo_{0.75}$, and molybdenum are indicated.

tent. Thus a Kohn anomaly corresponding to transitions across this surface should occur at progressively smaller values of ζ in the alloys, in agreement with the observations. This correlation is further evidence that these anomalies, in both the pure metal and the alloys, arise from the Kohn effect.

Two anomalies can be seen on the $\Lambda_1(F)$ branch of molybdenum (Fig. 8). The weaker one at $\zeta = 0.27$ is believed to arise from transitions a-b across the hole surface at H in Fig. 11. As in the case of niobium, this hole surface arises from the intersection of the Fermi level and the F_1 electron band, but since the molybdenum Fermi level is at a higher energy, the anomaly is expected to appear at a smaller phonon wave vector. The radius of the H hole surface in the [111] direction

is deduced to be 0.47 $Å^{-1}$ from the observed position of this anomaly, in reasonable agreement with the calculated Fermi surface.

A very pronounced decrease in frequency on the F_1 branch in pure molybdenum occurs at $\zeta \sim 0.96$. This anomaly may arise from electron transitions c-d in Fig. 11; its observed position agrees well with that predicted. Using the observed position of this anomaly together with the one observed at $\zeta = 0.27$, the radius of the Γ electron surface in the [111] direction is deduced to be 0.34 $Å^{-1}$, in reasonable agreement with the calculated dimension. It is probable that the pronounced decrease in frequency on the Δ branches near H also results from these transitions. In $Nb_{0.09}$-$Mo_{0.91}$ (Fig. 7) this anomaly on the F_1 branch has moved to $\zeta \sim 0.93$ and has become
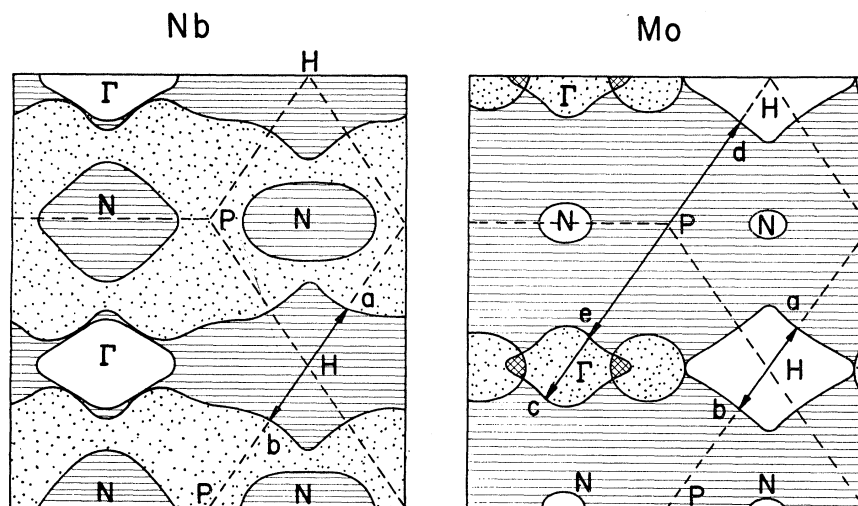
FIG. 11. (110) sections of the calculated (see Ref. 20) Fermi surfaces of niobium and molybdenum. The arrows indicate possible electronic transitions which correlate with anomalies on the experimental dispersion curves.

weaker, while in $Nb_{0.25}$-$Mo_{0.75}$ it was not observed. This shift in the position of the anomaly is in agreement with the band-structure calculations.

A weak anomaly is observed on the F_1 branch of pure molybdenum at $\zeta \sim 0.78$. This is the approximate position expected for an anomaly arising from e-d transitions assuming the other assignments are correct. In the Mo-rich alloys, some structure is evident in this region but it is not sufficiently well established to make any quantitative deductions.

From the electronic band structure shown in Fig. 10 it can be seen that, as the molybdenum content of the alloys increases, the Fermi energy rises above the Γ_{25}' electronic level. This occurs in alloys which contain approximately 34at.% Nb. Anomalies seem to be weakest near this composition, and no sudden change is observed in the dispersion curves on passing through it. From Fig. 9, however, it can be seen that the H_{15} frequency has a maximum at approximately this composition.

5. CONCLUSIONS

Measurements at 296°K of the normal-mode frequencies of the transition metals niobium and molybdenum, and of six of their alloys have been described. The phonon dispersion curves are found to be very different for the two pure metals, and, from the results for the alloys, it is seen that the variation of the dispersion curves with composition is complicated, involving changes of shape as well as general frequency level. The changes in shape are closely related to the electronic band structure. The behavior of the dispersion curves as a function of composition is very different near the extremes of composition. The Nb-rich alloys increase their general level of frequencies significantly with increasing molybdenum content while the shape of their dispersion curves remains substantially unchanged. The Mo-rich alloys appear to have a very different type of behavior. The general level of frequencies is nearly constant while the shape of the curves is very sensitive to alloy composition.

Fourier analysis of the individual branches of the dispersion curves shows that the interatomic forces are of very long range and that the long-range Fourier coefficients oscillate in sign. These oscillations can arise as a result of singularities in the electron dielectric function. Such singularities in the dielectric function also cause anomalies to appear on the dispersion curves and attempts have been made to interpret the observed anomalies in terms of this effect (the Kohn effect). With the aid of a calculated electronic band structure for tungsten together with the assumption of rigid electron bands, many of the observed kinks on the dispersion curves have been correlated with the Fermi surface. This correlation is further evidence that the phonon dispersion curves are determined to a large extent by the electronic structure of these metals. It provides support for the validity of the rigid-band model in this alloy system, and indicates that observation of Kohn anomalies may be a useful technique for Fermi surface measurements in disordered alloys.

Despite the correlation of several features of the dispersion curves with the electronic band structure, the phonon dispersion in these metals and alloys is not understood in any fundamental respect. This can only be achieved when a satisfactory theoretical model relating the phonon dispersion curves and the electronic band structure is available.

ACKNOWLEDGMENTS